C. R. Physique 11 (2010) 531–540

Contents lists available at ScienceDirect

Comptes Rendus Physique

www.sciencedirect.com

Interactions between radiofrequencies signals and living organisms

Whole body exposure at 2100 MHz induced by plane wave of random incidences in a population

Estimation du niveau d'exposition d'une population à une onde plane à 2100 MHz d'incidence aléatoire

Emmanuelle Conil [a,b,∗], Abdelhamid Hadjem [a,b], Aimad El Habachi [a,b], J. Wiart [a,b]

[a] *Orange Labs, R&D, 38-40, rue du Général Leclerc, 92794 Issy-les-Moulineaux, France*
[b] *WHIST Lab, Issy-les-Moulineaux, France*

ARTICLE INFO

Article history:
Available online 3 January 2011

Keywords:
Dosimetry
Finite-difference time-domain method
Highlighted surface
Plane waves
Specific absorption rate

Mots-clés :
Dosimétrie
Méthode des différences finies en domaine temporel
Surface en évidence
Ondes planes
Taux d'absorption spécifique

ABSTRACT

In this article, the whole body exposure induced by plane wave coming from a random direction of arrival is analyzed at 2100 MHz. This work completes previous studies on the influence of different parameters on the whole body exposure (such as morphology, frequency or usage in near field). The Visible Human phantom has been used to build a surrogate model to predict the whole body exposure depending on the highlighted surface of the phantom and on the direction of arrival of the incident plane wave. For the Visible Human, the error on the whole body averaged Specific Absorption Rate (SAR) is on average 4%. The surrogate model is applied to other 3D anthropomorphic phantoms for a frontal incidence with an averaged error of 10%. The great interest of the surrogate model is the possibility to apply a Monte Carlo process to assess probability distribution function of a population. A recent French anthropometric database of more than 3500 adults is used to build the probability distribution function of the whole body SAR for a random direction of arrival.

RÉSUMÉ

Le niveau d'exposition des personnes aux ondes électromagnétiques est influencé par différents paramètres comme la morphologie, la posture ou la fréquence de l'onde. De nombreuses études ont été menées afin de quantifier l'influence de ces différents paramètres. Très souvent, la direction d'arrivée de l'onde est fixée de façon déterministe. Or en réalité, les ondes proviennent de directions aléatoires autour du plan horizontal. Dans cette étude, les ondes incidentes se situent dans le plan horizontal et la fréquence utilisée est 2100 MHz. La direction d'arrivée de l'onde incidente est considérée comme une variable aléatoire. Une étude de dosimétrie numérique a été menée sur le fantôme *Visible Human* pour construire un modèle réduit permettant de prédire le débit d'absorption spécifique (DAS) corps entier en fonction de l'angle d'incidence et de paramètres morphologiques. Le modèle réduit induit une erreur de 4% en moyenne sur le DAS corps entier. Ce modèle est ensuite appliqué à d'autres fantômes anthropométriques (10 adultes dont 3 femmes) pour une incidence fixée. L'erreur moyenne sur les 10 modèles est de 10% sur le DAS corps entier. Finalement, le modèle réduit est utilisé de façon à estimer la distribution du DAS corps entier dans une population donnée. Une base de données anthropométriques de plus

∗ Corresponding author at: Orange Labs, R&D, 38-40, rue du Général Leclerc, 92794 Issy-les-Moulineaux, France.
E-mail address: emmanuelle.conil@orange-ftgroup.com (E. Conil).

1631-0705/$ – see front matter
doi:10.1016/j.crhy.2010.11.007

de 3500 adultes a été utilisée afin de construire la distribution du DAS corps entier induit par une onde plane à 2100 MHz d'incidence aléatoire dans le plan horizontal.

1. Introduction

Electromagnetic waves are nowadays intensively used in particular by wireless communication systems such as cellular base stations, mobile phones and WiFi systems. Because of that, much effort is dedicated to the Electromagnetic Fields exposure assessment. To protect people against overexposure from electromagnetic waves, the International Committee on Non-Ionizing Radiation Protection and the IEEE have recommended limits [1,2]. In all cases the fundamental limits are given by the basic restrictions that are limiting the Specific Absorption Rate (SAR expressed in W/kg). The SAR assessment requires complex laboratory equipments; because of this ICNIRP and IEEE have also defined derived limits: the reference levels that limit the electromagnetic field strength to guarantee compliance with the basic restrictions. Simplified human models such as ellipsoids have been used to define these limits.

Numerical dosimetry to assess the exposure to EMF is being strongly developed since 10 years thanks to the great progress in computing systems. Most of the time, numerical dosimetry studies are considering the exposure of a model of a human in one configuration. However, since a few years ago, the community is dealing with the variability of human beings and of exposure configurations. The new challenge is to include this variability in the numerical study as incertitude. Different kinds of variability can be distinguished. In [3] and [4], the influence of the morphology of the human models is analyzed. Refs. [5] and [6] are dealing with the influence of the near field exposure conditions. In [7] the influence of far field exposure conditions is analyzed.

In this article, based on the analysis performed in [8], we complete the surrogate model established to predict the whole body exposure induced by a plane wave for different directions of arrival. The surrogate model presents the great advantage of not requiring heavy numerical simulation as is usual in numerical dosimetry. The model is used to estimate the distribution of the whole body SAR, induced by an arbitrary horizontal plane wave, vertically polarized, in the French population.

The second section is dedicated to the construction of the surrogate model. In the third section, the surrogate model is intensively used to estimate the distribution of the whole body averaged SAR in the French population.

2. Predictive model of the exposure induced by a plane wave

2.1. Illustration of the exposure induced by plane waves with different angles of arrival

Far field exposure is considered in this article. Sources of exposure are simulated by plane waves, vertically and horizontally polarized. Since a few years, the region around 2 GHz is becoming of interest because of the development of wireless technologies around 2 GHz (such as GSM, UMTS or WiFi). Moreover, previous works [8–12] have shown that around 2 GHz, the reference levels might be not conservative in particular for women and children.

The higher the frequency, the more the absorption by a human body is superficial, and in this way, the power absorbed by the human body is strongly correlated to the illuminated surface. This relationship has been already analyzed in [4, 8–10], but for few angles of arrival and from the normative point of view. Nowadays the challenge is not only to check compliance, but even more to assess the exposure of an entire population in real conditions of exposure. In [4], the influence of morphology on the exposure has been statistically analyzed in one configuration of exposure (2100 MHz and frontal incidence). In a real environment, the waves are coming from all azimuth angles. In [8], we focused on the exposure in the horizontal and $\pm 20^\circ$ tilted planes for the entire azimuth, with 10° steps (see Fig. 1).

In this first analysis, the Visible Human model [13] has been chosen to illustrate the behavior of the whole body exposure depending on the direction of arrival of the horizontal incident plane wave. Both horizontal and vertical polarizations in isolated conditions have been considered at 2100 MHz. Fig. 2 shows the preliminary results presented in [8]. The whole body SAR induced at 2100 MHz in the Visible Human shows a periodic shape depending on the azimuth angle, especially for the V-polarization.

Complementary simulations confirm this behavior at 2400 MHz as shown on Fig. 3.

Concerning the H-polarization, a flat zone appears around the back exposure (azimuth $= 180^\circ$) disturbing the periodic shape of the whole body exposure. This flat zone can be explained by the geometry of the Visible Human model. The back of the Visible Human is very flat because he was in a dorsal decubitus position when the model has been constructed. From now, the analysis will be focused on the vertical polarization.

In real environment, far field exposure is mainly due to plane waves coming from angles around the horizontal. Fig. 4 illustrates the variation of the whole body exposure of the Visible Human at 2100 MHz for plane waves arriving in a vertical plane with elevations from -90° to $+90^\circ$ and a vertical polarization. A periodic behavior is also demonstrated.

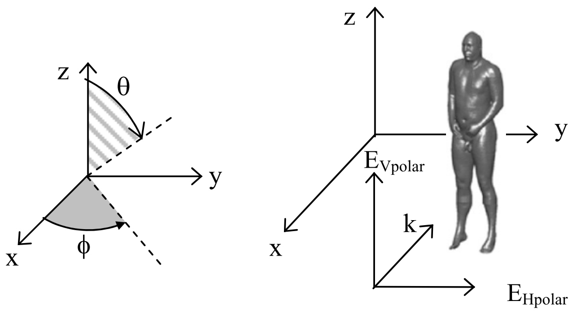

Fig. 1. Condition of exposure – plane wave at 2100 MHz in isolated conditions with different directions of arrival (theta = 90° ± 20° and phi = [0 : 10 : 360]).

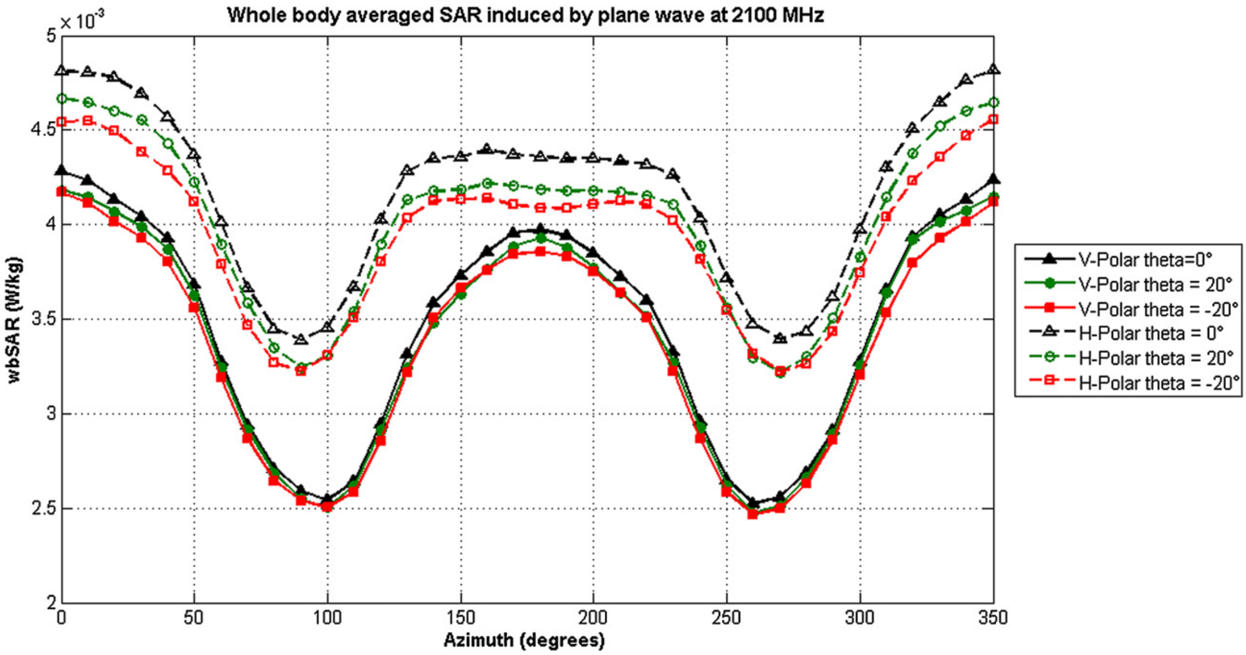

Fig. 2. Whole body SAR induced in VH at 2100 MHz for both V- and H-polarizations and the three elevation angles depending on the angle of arrival in azimuth.

2.2. Parametric model to predict whole body exposure

As previously mentioned, the absorption by the human body at high frequencies is mainly superficial. In [4,10–12], a good correlation between the absorbed power and the highlighted surface has been found for different anatomical phantoms and for few angles of arrival. The correlation between the whole body exposure and the highlighted surface is depending on different parameters, such as the morphology of the human model, the frequency and the azimuth angle. In [8], we described this correlation for one anthropomorphic model (the Visible Human) and one frequency 2100 MHz. First of all, the construction of the surrogate model is described considering the whole body exposure of the Visible Human, the frequency of 2100 MHz, the vertical polarization and horizontal directions of arrival from 0° to 360°.

In the configurations described in Section 2, two different ways have been considered to assess the highlighted surface of the Visible Human depending on the direction of arrival. The first one consists in calculating the surface projected along the direction of arrival. The second one is based on an approximation of the Visible Human by an ellipsoid. The height of the equivalent ellipsoid is the height of the Visible Human, and the two other axes are the width of shoulder and the depth at the waist as illustrated on Fig. 5.

Fig. 6 shows the highlighted surface of the Visible Human depending on the direction of arrival calculating by projection of the anthropomorphic model (continuous lines) and by considering the Visible Human as an ellipsoid (dashed lines). The same periodical behavior as the whole body exposure is observed.

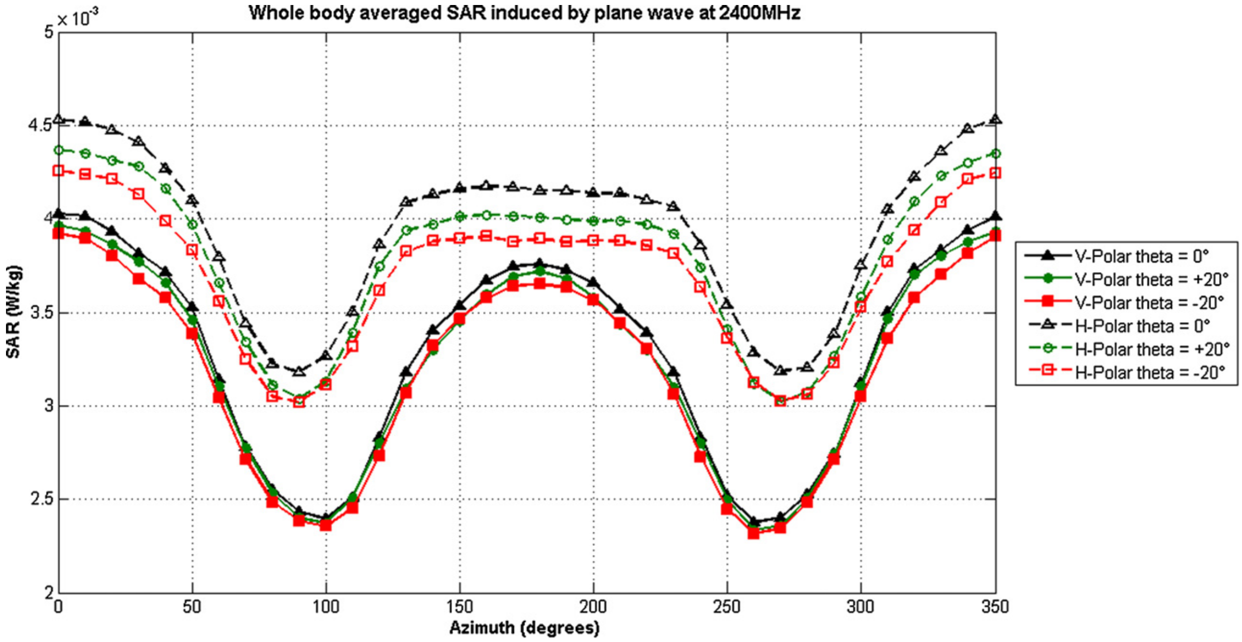

Fig. 3. Whole body SAR induced in VH at 2400 MHz for both V- and H-polarizations and the three elevation angles depending on the angle of arrival in azimuth.

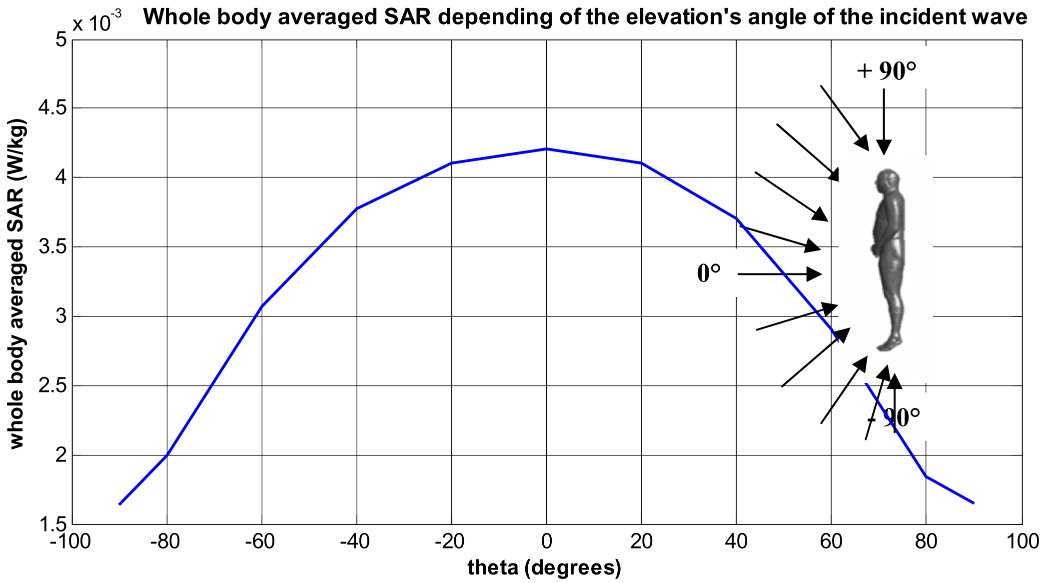

Fig. 4. Whole body SAR induced in VH at 2100 MHz for V-polarization depending on the angle of arrival in a vertical font plane.

Based on these observations, a surrogate model is proposed to predict the whole body SAR induced by a plane wave in a horizontal plane vertically polarized in isolated conditions depending on the azimuth angle. The model traduces that the absorbed power is linearly correlated to the highlighted surface (Eq. (1)):

$$\mathrm{SAR} = 0.75 \times \frac{\mathrm{surface}}{\mathrm{mass}} \times \mathrm{DSP} \tag{1}$$

The coefficient 0.75 is obtained from a Kolmogorov–Smirnov test, showing that the ratio between the SAR and the surface/mass can be described by a normal law with a mean of 0.75 and a standard deviation of 0.032 as illustrated on Fig. 7.

The DSP is the spectral density of power of the plane wave. The mass is calculated by assuming a mean density ρ in the equivalent ellipsoid of 1000 kg/m^3 (Eq. (2)).

$$\mathrm{mass} = \mathrm{volume} \times \rho \tag{2}$$

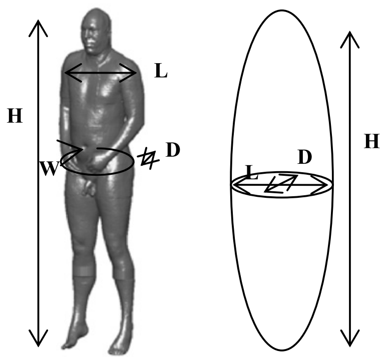

Fig. 5. Visible Human and the equivalent ellipsoid used to assess the highlighted surface.

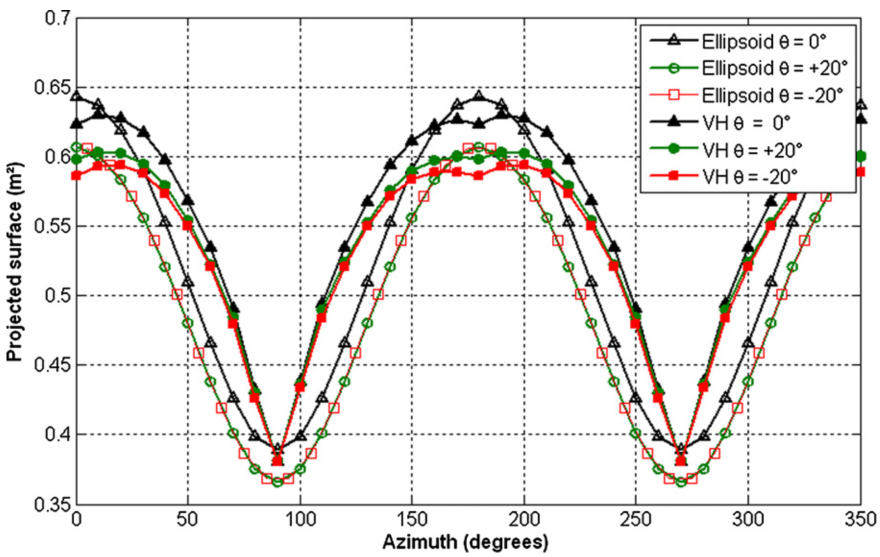

Fig. 6. Highlighted surface computed by projection of the VH model (continuous lines) or by using the equivalent ellipsoid (dashed lines).

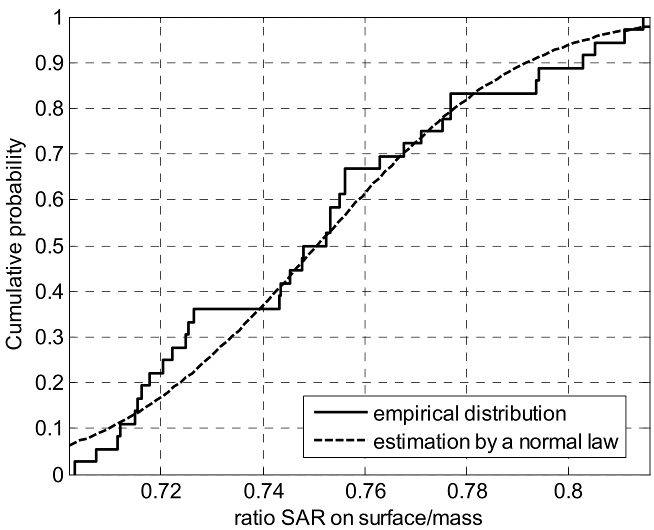

Fig. 7. Cumulative density function of the ratio between the whole body SAR and the ratio surface on mass calculated on the equivalent ellipsoid for all the V-polarization simulations. Empirical distribution is correctly described by a normal law.

The volume and the highlighted surface of the equivalent ellipsoid are analytically expressed in function of parameters H, L, P and ϕ representing respectively the height, the width shoulder, the depth at the waist of the phantom and the direction of arrival of the incident plane wave in the horizontal plane (Eqs. (3) and (4)).

$$\text{volume} = \frac{4}{3}\frac{H \times L \times P}{8} \tag{3}$$

$$\text{surface} = \pi \frac{H}{2}\sqrt{\left(\frac{L}{2}\right)^2 \cos(\Phi)^2 + \left(\frac{P}{2}\right)^2 \sin(\Phi)^2} \tag{4}$$

Finally, an analytical surrogate model is given for the whole body SAR by Eq. (5).

$$\text{SAR} = 0.75 \times \frac{\pi \sqrt{(\frac{L}{2})^2 \cos(\Phi)^2 + (\frac{P}{2})^2 \sin(\Phi)^2}}{\frac{1}{3} L \times P \times \rho} \times \text{DSP} \tag{5}$$

For the Visible Human phantom, the error associated to this surrogate model is between −6% and +10% depending on the azimuth angle. The averaged error on all the azimuth angles is 4%. Now we are going to analyze how to extend this analytical surrogate model to others phantoms than the Visible Human phantom.

3. Statistics on the predictive model

3.1. Deterministic cases on available 3D adult phantoms

First of all, we are going to apply the surrogate model built in previous section (Eq. (5)) to assess the whole body SAR induced in different 3D anthropomorphic models of adults for a frontal incidence. In this way, the robustness of the parametric model in function of the morphology is determined for a given direction of arrival. 3D anthropomorphic phantoms are built from MRI images or from high resolution color slice images. Worldwide several human phantoms models have been developed. 7 male and 3 female phantoms are used to test the surrogate model (Fig. 8). The phantoms have initial sizes of segmentation between 1 mm and 3.6 mm but all of them have been remeshed at 2 mm to test the surrogate model. Male models are the male of the Virtual family (Duke) [14], a Korean model (HDRK) [15], the UK model Norman [16], the Japanese man [17], the Korean ETRI model [18], the Zubal model [19] and the Visible Human model [13]. Female models are the female of the Virtual Family (Ella) [14], the UK female Naomi [20] and the Japanese woman [17].

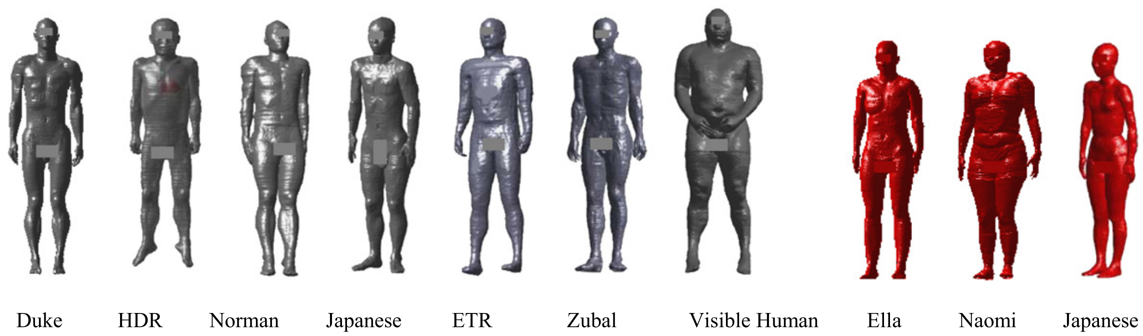

Fig. 8. Illustration of the 3D heterogeneous models of adults used to validate the parametric model.

The surrogate model induces an error between +6% and −22% on the whole body SAR for a frontal incidence if the Korean ETRI model is excluded (Fig. 9). The Korean ETRI model is particular in so far as it presents a skin very thick due to the initial size of segmentation. The thick skin protects the model artificially (in reality the skin is much thinner) and so the whole body SAR induced in the Korean ETRI model is much lower than for other similar models. The surrogate model is then not accurate in this specific case.

On average, the error on the whole body SAR induced by the variability of the morphology is of 10% for a given incidence (the frontal one) that is acceptable. Internal morphology has an influence on the exposure but it is very difficult to take into account because of the lack of data on internal morphology as detailed on [4].

3.2. Statistics on the French population

The main interest of analytical surrogate model is the possibility to use it intensively to obtain the distribution of the whole body exposure of a given population characterized by morphological parameters. Recently, a measurements campaign on a random part of the French population has been made. The sample is constituted of 2244 women aged from 17 to 83

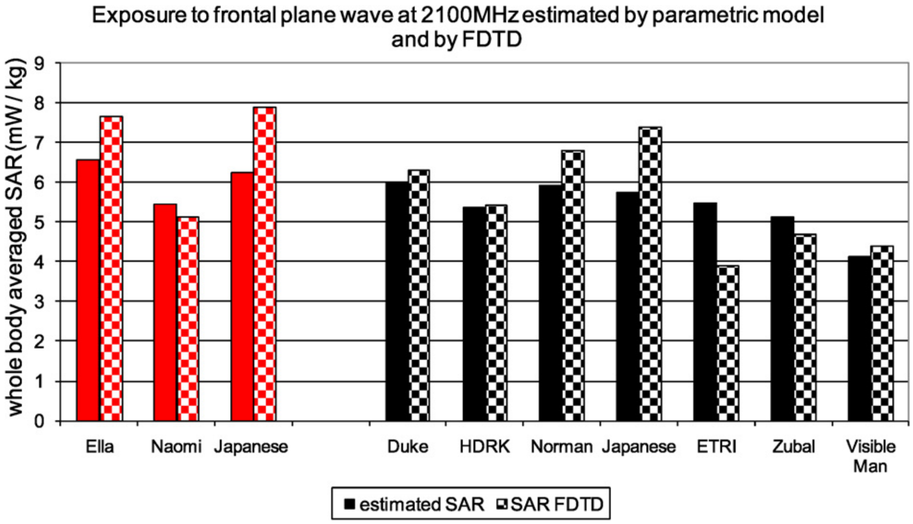

Fig. 9. Whole body SAR induced by frontal plane wave at 2100 MHz (1 W/m^2) for different adult models computed either by the parametric model (full bars) or by the FDTD (squared bars).

and 1643 men aged from 17 to 84. The size of the database enables to assume that the sample is representative of the French adult population.

The shoulder breadth has been collected in this database but not the depth at the waist. However, the waist size has been collected and by using the equivalent ellipsoid, the waist size is assimilated to the perimeter of the ellipsoid. By that way, the depth P at the waist is deduced from the waist size W and the shoulder width L (Eq. (6)) by using the Kepler approximation to compute the perimeter.

$$W = \pi\sqrt{L \times P} \to P = \frac{W^2}{\pi^2 \times L} \tag{6}$$

By replacing P by the formula (Eq. (6)) in the formula of the SAR (Eq. (5)), we obtain a formula of the SAR in function of L, W and ϕ the shoulder width, the waist size and the direction of arrival of the incident plane wave respectively.

$$\mathrm{SAR} = 0.77 \times \frac{\pi\sqrt{(\frac{L}{2})^2\cos(\Phi)^2 + (\frac{W^2}{2\pi^2 \times L})^2\sin(\Phi)^2}}{\frac{1}{3} \times \frac{W^2}{\pi^2} \times \rho} \times \mathrm{DSP} \tag{7}$$

From the anthropomorphic database, parametric laws are used to estimate the probability density function of the shoulder width L and the waist size W (see Fig. 5). The criterion used for selecting the appropriate law of these densities is the maximum likelihood [21].

Lognormal laws are used to estimate L and W (Fig. 10).

Moreover, the anthropomorphic database points out a correlation between the shoulder width and the waist size characterized by a correlation factor of 0.67. A sample of L and W is generated by a Monte Carlo process taking into account the correlation. The whole body exposure is computed for this sample by using the analytical surrogate model (Eq. (7)). First of all, we consider a deterministic direction of arrival either a frontal incidence ($\phi = 0$) or an aside incidence ($\phi = \pi/2$). The probability density functions of the whole body SAR obtained are shown on Fig. 11. As expected, the whole body SAR is higher for frontal exposure than for the aside exposure. The whole body SAR distribution is much more spread in the case of frontal exposure than in the case of aside exposure. The distributions of the morphological factors (Fig. 10) explain this behavior. The distribution of the shoulder width is rather thin when that of the waist size is more spread.

However, in the real environment, waves are coming from any azimuth angle. So the direction of arrival is now considered as a random uniform variable between 0 and 2π. Fig. 12 shows the density distribution function of the whole body SAR induced in the sample of the French population for random azimuth angle. By using a random azimuth angle, the probability density function is becoming more flat than for a given direction of arrival.

From these distributions of whole body SAR, the quintiles at 95% have been extracted to give an upper bound of the exposure of the studied population (Table 1).

4. Conclusion

In this article, the correlation between the whole body exposure and the highlighted surface is analyzed. This correlation is depending on the morphology of the phantom, on the frequency, on the polarization and on the azimuth angle. A set

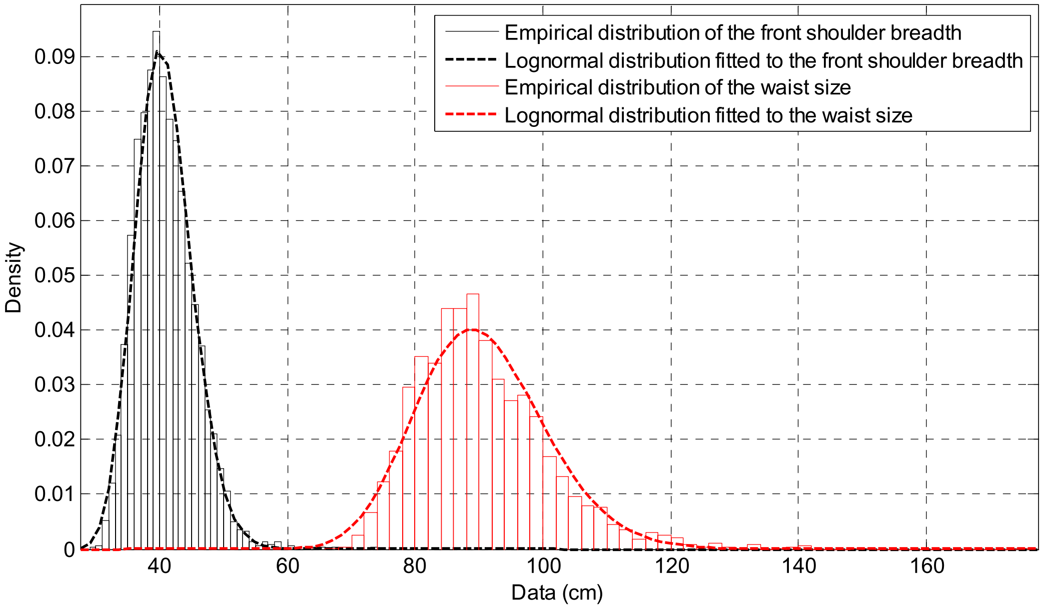

Fig. 10. Estimation of empirical density function of the shoulder width L and the waist size W by lognormal laws.

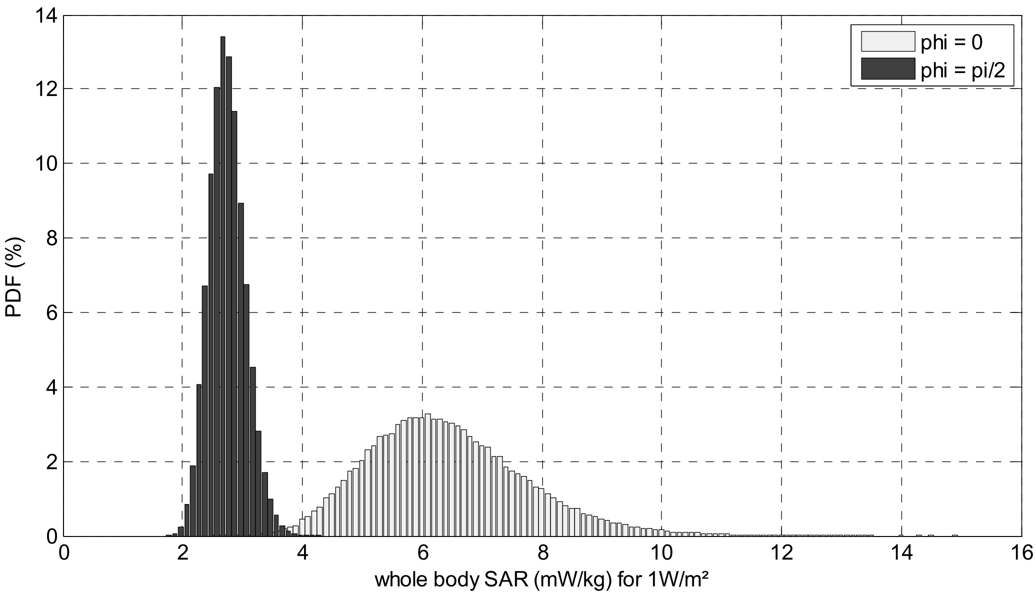

Fig. 11. Probability density function of the whole body SAR induced in the French adult population for frontal (dark PDF) and aside (light PDF) directions of arrivals.

of simulations performed with the Finite Difference Time Domain method have been used to build an analytical model of the whole body exposure induced in the Visible Human. This model has been built at 2100 MHz and is depending on morphological factors (the shoulder width and the dept at waist) and on the direction of arrival in the case of V-polarized plan waves in horizontal plane. The simulations have shown that the dependence with the azimuth angle of the whole body SAR induced in the Visible Human is the same as the one of the highlighted surface of the phantom. The dependence is periodic with the azimuth angle. The relationship is of greater agreement for V-polarization than for H-polarization by construction of the Visible Human model. For V-polarization, the incertitude on the prediction of the exposure of the Visible Human is only 4% in averaged on all the azimuth angles. The proportionality coefficient is frequency dependent. The higher the frequency, the more the absorption is superficial. The study has been led at 2100 MHz but complementary simulations have confirmed the proportionality at 2400 MHz but with another coefficient. Further works would analyze the frequency dependence of the proportionality between whole body exposure and highlighted surface.

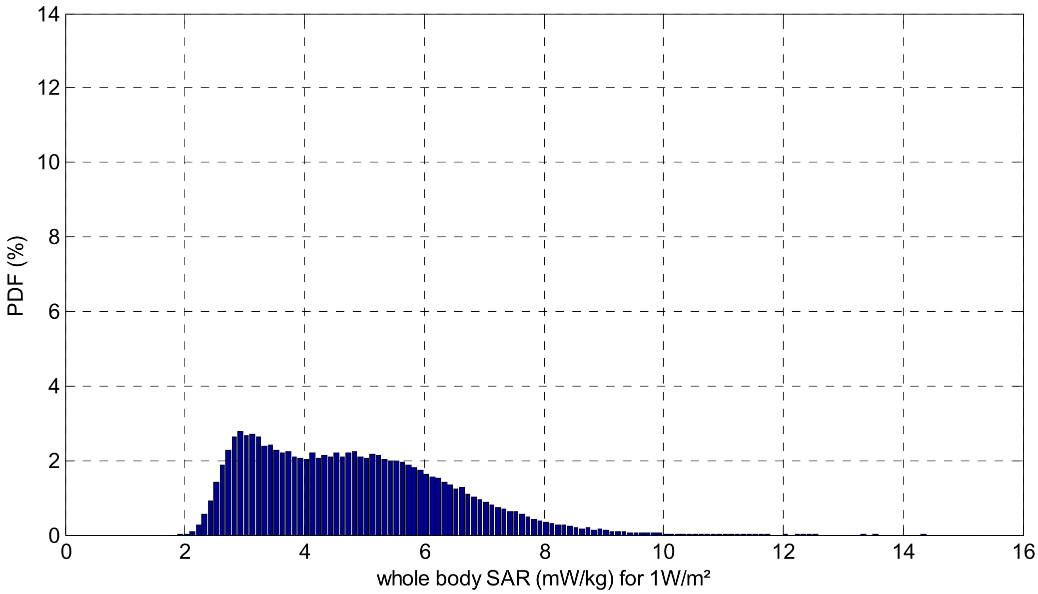

Fig. 12. Probability density function of the whole body SAR induced in the French adult population for random azimuth angle.

Table 1
Quantiles at 95% of the whole body SAR induced in the studies population for frontal, aside and random incidences.

	SAR@95% (mW/kg)
$\Phi = 0$	9
$\Phi = \pi/2$	3.4
Φ random in $[0\ 2\pi]$	7.8

Concerning the influence of the morphology, the analytical model has been tested on other 3D anthropomorphic models in one configuration (frontal exposure). On 8 adult phantoms, the mean error is only 4% and maximal error is 20%.

The great interest of such a model is the possibility to use Monte Carlo process to estimate the distribution of the whole body exposure of a population. Based on a recent anthropomorphic database of 3887 French adults, the probability distribution function of the whole body SAR induced by plane waves with random direction of arrivals in the horizontal plane is assessed.

Acknowledgements

The authors would like to thank Dr. S. Watanabe from NICT, Japan, Dr. A.K. Lee from ETRI, Korea, Dr. P.J. Dimbylow from HPA, UK, Dr. P. Mason, Dr. J. Ziriax from Brook'AF, US, Pr. Zubal from Yale University, USA and Dr. N. Kuster from Itis to have provided human body models.

This study has been supported by the French ANR project MULTIPASS (http://multipass.elibel.tm.fr/).

References

[1] ICNIRP, Guidelines for limiting exposure to time-varying electric, magnetic and electromagnetic fields (up to 300 GHz), Health Phys. 44 (1998) 1630–1639.
[2] IEEE Std C95.1 – 2005, IEEE standard for safety levels with respect to human exposure to radio frequency electromagnetic fields, 3 kHz to 300 GHz.
[3] E. Conil, A. Hadjem, F. Lacroux, M.F. Wong, J. Wiart, Variability analysis of SAR from 20 MHz to 2400 MHz for different adult and child models using FDTD, Phys. Med. Biol. 53 (6) (March 2008) 1511–1525.
[4] A. El Habachi, E. Conil, A. Hadjem, E. Vazquez, M.F. Wong, A. Gati, J. Wiart, Statistical analysis of whole-body absorption depending on anatomical human characteristics at a frequency of 2.1 GHz, Phys. Med. Biol. 55 (1) (January 2010) 1875–1887.
[5] A. Hadjem, E. Conil, A. Gati, M.F. Wong, J. Wiart, Analysis of power absorbed by children's head as a result of new usages of mobile phone, IEEE EMC 52 (4) (November 2010) 812–819.
[6] O. Aiouaz, D. Lautru, M.-F. Wong, E. Conil, A. Gati, J. Wiart, V. Fouad Hanna, Uncertainty analysis of the specific absorption rate induced in a phantom using a stochastic spectral collocation method, Annales des telecommunications, submitted for publication.
[7] T. Kientega, E. Conil, A. Hadjem, A. Gati, E. Richalot, M.F. Wong, O. Picon, J. Wiart, Assessment of the SAR induced by multiple plane waves exposure, Annales des telecommunications, submitted for publication.
[8] E. Conil, A. Hadjem, A. Gati, M.F. Wong, J. Wiart, Influence of plane wave incidence angle on whole body and local exposure at 2100 MHz, IEEE EMC, doi:10.1109/TEMC.2010.2061849.

[9] J. Wiart, E. Conil, A. El Habachi, A. Hadjem, M.F. Wong, Influence of morphology on RF human exposure, in: International Symposium on EMC, Kyoto, 20–24 July 2009.
[10] A. Hirata, S. Kodera, J. Wang, O. Fujiwara, Dominant factors influencing whole-body average SAR due to far-field exposure in whole-body resonance frequency and GHz regions, Bioelectromagnetics 28 (6) (Sept. 2007) 484–487.
[11] S. Kühn, W. Jennings, A. Christ, N. Kuster, Assessment of induced radio-frequency electromagnetic fields in various anatomical human body models, Phys. Med. Biol. 54 (Jan. 2009) 875–890.
[12] Hirata, Y. Nagaya, F. Osamu, A.T. Nagaoka, S. Watanabe, Correlation between absorption cross section and body surface area of human for far field exposure at GHz bands, in: Proc. IEEE Int. Symp. on EMC, Qingdao, China, Oct. 2007.
[13] M.J. Ackerman, Accessing the visible human project, D-Lib Mag [online], available: http://www.nlm.nih.gov/research/visible/visible_human.html, Oct. 1995.
[14] ITIS Foundation, http://www.itis.ethz.ch/index/index_humanmodels.html.
[15] C.H. Kim, S.H. Choi, J.H. Jeong, C. Lee, M.S. Chung, HDRK-Man: a whole-body voxel model based on high-resolution color slice images of a Korean adult male cadaver, Phys. Med. Biol. 53 (15) (Aug. 2008) 4093–4106.
[16] P.J. Dimbylow, The development of realistic voxel phantoms for electromagnetic field dosimetry, in: Proc. Int. Workshop on Voxel Phantom Development (National Radiological Protection Board), Chilton, UK, 1995, pp. 1–7.
[17] T. Nagaoka, S. Watanabe, K. Sakurai, E. Kunieda, S. Watanabe, M. Taki, Y. Yamanaka, Development of realistic high-resolution whole-body voxel models of Japanese adult males and females of average height and weight, and application of models to radio-frequency electromagnetic-field dosimetry, Phys. Med. Biol. 49 (1) (Dec. 2004) 1–15.
[18] Ae.-K. Lee, W.Y. Choi, M.S. Chung, H.-D. Choi, J.-I. Choi, Development of Korean male body model for computational dosimetry, ETRI Journal 28 (1) (Feb. 2006) 107–110.
[19] I.G. Zubal, C.R. Harrell, E.O. Smith, A.L. Smith, Two dedicated voxel-based anthropomorphic (torso and head) phantoms, in: Proc. Int. Workshop on Voxel Phantom Development (National Radiological Protection Board), Chilton, UK, 1995, pp, 105–111.
[20] P.J. Dimbylow, Development of the female voxel phantom, NAOMI and its application to calculations of induced current densities and electric fields from applied low frequency magnetic and electric fields, Phys. Med. Biol. 50 (6) (March 2005) 1047–1070.
[21] G. Saporta, Probabilités, analyse de données et statistiques, Gulf Publishing Company, January 1990.